Insect lipoprotein follows a transferrin-like recycling pathway that is mediated by the insect LDL receptor homologue

Dennis Van Hoof*, Kees W. Rodenburg and Dick J. Van der Horst

Department of Biochemical Physiology and Institute of Biomembranes, Utrecht University, Padualaan 8, 3584 CH Utrecht, The Netherlands
*Author for correspondence (e-mail: d.vanhoof@bio.uu.nl)

Summary

The lipoprotein of insects, high-density lipophorin (HDLp), is homologous to that of mammalian low-density lipoprotein (LDL) with respect to its apolipoprotein structure. Moreover, an endocytic receptor for HDLp has been identified (insect lipophorin receptor, iLR) that is homologous to the LDL receptor. We transfected LDL-receptor-expressing CHO cells with iLR cDNA to study the endocytic uptake and intracellular pathways of LDL and HDLp simultaneously. Our studies provide evidence that these mammalian and insect lipoproteins follow distinct intracellular routes after receptor-mediated endocytosis. Multicolour imaging and immunofluorescence was used to visualize the intracellular trafficking of fluorescently labeled ligands in these cells. Upon internalization, which can be completely inhibited by human receptor-associated protein (RAP), mammalian and insect lipoproteins share endocytic vesicles. Subsequently, however, HDLp evacuates the LDL-containing endosomes. In contrast to LDL, which is completely degraded in lysosomes after dissociating from its receptor, both HDLp and iLR converge in a non-lysosomal juxtanuclear compartment. Colocalization studies with transferrin identified this organelle as the endocytic recycling compartment via which iron-depleted transferrin exits the cell. Fluorescently labeled RAP is also transported to this recycling organelle upon receptor-mediated endocytosis by iLR. Internalized HDLp eventually exits the cell via the recycling compartment, a process that can be blocked by monensin, and is re-secreted with a $t_{1/2}$ of ~13 minutes. From these observations, we conclude that HDLp is the first non-exchangeable apolipoprotein-containing lipoprotein that follows a transferrin-like recycling pathway despite the similarities between mammalian and insect lipoproteins and their receptors.

Key words: Lipophorin, Low-density lipoprotein, LDL receptor, RAP, Transferrin, Endocytosis, Recycling

Introduction

The extracellular transport of water-insoluble lipids through the aqueous circulatory system of animals is mediated by lipoproteins. Mammals rely on a wide array of lipoproteins with various compositions and functions. Insects, however, use a single type of lipoprotein, high-density lipophorin (HDLp), to effect the transport of a variety of hydrophobic molecules through the blood (hemolymph) (Soulages and Wells, 1994; Ryan and Van der Horst, 2000; Van der Horst et al., 2002). In several aspects, HDLp is comparable to low-density lipoprotein (LDL), the predominant transporter of cholesterol in mammals. LDL comprises a single non-exchangeable apolipoprotein, apoB, that is produced by the liver as a large, monomeric protein of 4536 amino acids (Shelness and Sellers, 2001). The protein component of HDLp also consists of non-exchangeable apolipoprotein, apolipophorin (apoLp)-I and -II, which are derived through post-translational cleavage from a common precursor protein of 3359 amino acids, synthesized in the fat body (Weers et al., 1993; Bogerd et al., 2000). Sequence and domain structure analysis indicate that this insect precursor protein and apoB are homologous and have emerged from an ancestral gene (Babin et al., 1999; Mann et al., 1999; Segrest et al., 2001).

Uptake of LDL is mediated by the LDL receptor (LDLR), which is the prototype for a large class of endocytic transmembrane receptors (Brown et al., 1997; Hussain et al., 1999). Endocytosis of LDL has been extensively investigated and shown to result in the degradation of the complete lipoprotein particle in lysosomes (Goldstein et al., 1985; Brown and Goldstein, 1986; Dunn and Maxfield, 1992). Recently, a receptor expressed by the fat body of *Locusta migratoria* has been cloned and sequenced, and identified as a novel member of the LDLR family (Dantuma et al., 1999). This insect lipophorin receptor (iLR) was shown to mediate endocytic uptake of HDLp in transiently-transfected COS-7 cells. A characteristic feature of HDLp is its functioning as a reusable shuttle both at rest and during flight activity. Thus, the particle selectively loads and unloads lipids at target tissues, without concomitant degradation of HDLp (Van der Horst, 1990; Soulages and Wells, 1994; Ryan and Van der Horst, 2000; Van der Horst et al., 2001; Van der Horst et al., 2002). In apparent contrast to the concept of selective lipid uptake, however, during developmental stages of larval and young

adult locusts, receptor-mediated endocytic uptake of HDLp in the fat body was demonstrated (Dantuma et al., 1997). These authors additionally showed that incubation of fat body tissue with HDLp resulted in uptake of lipids, however, without substantial degradation of the apolipoprotein component. The involvement of an LDLR family member in lipoprotein metabolism implies complete lysosomal degradation of HDLp which is in disagreement with these findings. Thus far, the intracellular distribution after internalization of HDLp mediated by iLR had not been investigated. Therefore, the intriguing question remained to be answered whether this novel iLR, in contrast to all other LDLR family members, is able to recycle its ligand after internalization.

LDL, along with di-ferric transferrin (Tf), has been extensively used to study intracellular transport of ligands that are internalized by receptor-mediated endocytosis (Goldstein et al., 1985; Brown and Goldstein, 1986; Mellman, 1996; Mukherjee et al., 1997). Via clathrin-coated pits, the ligand-receptor complexes enter the cell in vesicles that subsequently fuse with tubulo-vesicular sorting endosomes. Due to mild acidification of the vesicle lumen, LDL dissociates from its receptor, but Tf merely unloads its two iron-ions and remains attached to the Tf receptor (TfR) (Mellman, 1996; Mukherjee et al., 1997). After repeated fusions with endocytic vesicles, sorting endosomes become inaccessible to newly internalized material. Whereas the released LDL particles are retained in the sorting endosome, most of the remaining membrane constituents (e.g. LDLR and TfR), enter the tubular extensions. The tubules bud off and are delivered to the morphologically distinct endocytic recycling compartment (ERC) (Yamashiro et al., 1984; Mayor et al., 1993; Mukherjee et al., 1997). Consequently, Tf accumulates in these large, long-lived, juxtanuclear vacuoles and, eventually, exits the compartments with a $t_{1/2}$ of ~7 minutes (Mayor et al., 1993; Ghosh et al., 1994). Sorting endosomes, however, mature into lysosomes in which LDL particles are completely degraded (Goldstein et al., 1985; Brown and Goldstein, 1986; Dunn et al., 1989).

In the present study, CHO cell lines, in which the intracellular LDL and Tf transport pathways are well characterized, were stably transfected with iLR cDNA. These transfected cells were used to analyze the distribution and sorting of internalized insect and mammalian ligands, simultaneously. Multicolour imaging allowed visualization of multiple fluorescently-labeled ligands after endocytic uptake with high temporal and spatial resolution. Incubation of iLR-transfected CHO cells with HDLp in combination with either LDL or Tf initially resulted in colocalization of the insect lipoprotein with LDL in sorting endosomes. However, in contrast to LDL that dissociates from its receptor, HDLp is efficiently removed from these vesicles and, together with iLR, accumulates in the Tf-positive ERC, as confirmed with immunofluorescence. In addition to HDLp, iLR is capable of binding and internalizing human receptor-associated protein (RAP), a ligand that is structurally unrelated to lipoproteins. Like HDLp, this ligand is transported to the ERC after receptor-mediated endocytosis. Similar to Tf, internalized HDLp is re-secreted from the cells with a $t_{1/2}$ of ~13 minutes and thereby escapes the lysosomal fate of endocytosed LDL particles. This provides the first example of an LDLR homologue that, in contrast to all the other family members, is able to recycle LDL-like lipoprotein upon receptor-mediated endocytosis.

Materials and Methods

Antibodies, reagents and proteins

Polyclonal rabbit-anti-iLR 9218 antibody was raised against a synthetic peptide representing the C-terminal 19 amino acids (865-883) of iLR (Dantuma et al., 1999), polyclonal rabbit-anti-apoLp-I and -II antibodies were raised against the apolipophorins as described by Schulz et al. (Schulz et al., 1987); rabbit-anti-LDLR 121 antibody was a gift from Ineke Braakman (Department of Bio-Organic Chemistry, Utrecht University, Utrecht, The Netherlands) human RAP was a gift from Michael Etzerodt (IMSB, Aarhus University, Aarhus, Denmark) and LysoTracker Yellow (Molecular Probes) was a gift from Arjan de Brouwer (Department of Biochemistry of Lipids, Utrecht University, Utrecht, the Netherlands). Geneticin (G-418) (GibcoBRL), precision protein standards prestained broad range marker (Bio-Rad), alkaline phosphatase-conjugated affinipure goat-anti-rabbit IgG (AP-GAR) and Cy5-conjugated goat-anti-rabbit IgG (Cy5-GAR) (Jackson ImmunoResearch Laboratories Inc.), leupeptin, aprotinin, monensin and nocodazole (Sigma), DiI(C$_{18}$(3)) (1,1′-dioctadecyl-3,3,3′,3′-tetramethylindocarbocyanine percholate), Oregon Green 488 carboxylic acid and tetramethylrhodamine-labeled Tf (Molecular Probes), saponin and iodine monochloride (ICN Biochemicals), BSA and cold water fish gelatin (Sigma), ^{125}I[iodine] (3.9 GBq/ml; Amersham Pharmacia Biochem) and chloramine-T (Merck) were obtained from commercial sources. Human LDL was isolated from blood plasma (Bloedbank Midden Nederland) as described by Redgrave et al. (Redgrave et al., 1975); HDLp was isolated from locust hemolymph by ultracentrifugation (Dantuma et al., 1996) with the following modifications to the original protocol. Hemolymph collected from 12-15 days old locusts that were reared under crowded conditions was directly diluted in ice-cold insect saline buffer supplemented with leupeptin (4 µg/ml) and aprotinin (4 µg/ml).

Cell culture

The CHO cells were cultured in 75 cm^2 polystyrene culture flasks (Nunc Brand Products) with growth medium containing HAM's F-10 Nutrient mixture, 10% heat inactivated fetal bovine serum, 100 U/ml penicillin G sodium and 100 µg/ml streptomycin sulphate in 85% saline (Gibco BRL) at 37°C in a humidified atmosphere of 5% CO$_2$. Growth medium of iLR-expressing cells was supplemented with 300 µg/ml G-418. For fluorescence microscopy and confocal laser scanning microscopy, cells were grown on 15 or 18-mm and 24-mm glass coverslips (Menzel-Gläser) in 12-wells (3.5 cm^2/well) and 6-wells (9.6 cm^2/well) multidishes (Nunc Brand Products), respectively.

Generation of CHO cell lines stably expressing iLR

Wild-type CHO cells were grown to ~40% confluency in 6-wells multidishes and transfected for 20 hours with 5 µg of piLR-e plasmid (Dantuma et al., 1999) DNA in 2 ml serum free growth medium supplemented with 20 µl Lipofectin reagent (Invitrogen Life Technologies) according to the supplier's protocol. The cells were grown for 7-10 days in selective growth medium, containing 400 µg/ml G-418, to obtain stably transfected cells. These cells were isolated by limited dilution to generate monoclonal cell lines and checked for iLR expression. Because variable levels of iLR expression were observed in the different cell lines, we used a monoclonal CHO(iLR) cell line that showed the highest expression level of iLR for the incubation experiments described in this study.

Western blot analysis of CHO cell membrane extracts

Cells were harvested from 75 cm^2 polystyrene flasks at ~80%

confluency, resuspended in CHAPS buffer (20 mM HEPES, 124 mM NaCl, 4.7 mM KCl, 2.5 mM $CaCl_2$, 2.5 mM Na_2HPO_4, 1.2 mM $MgSO_4$, 1 mM EDTA, 0.1 mM benzamidine, 1 µg/ml leupeptin, 1 µg/ml aprotinin, 1% CHAPS), incubated for 10 minutes on ice, and spun down at 15,000 g for 10 minutes at 4°C. Supernatant was diluted with 1 volume glycerol and soluble membrane proteins were either heated for 5 minutes at 95°C in Laemmli buffer (Laemmli, 1970) or directly dissolved in Laemmli buffer with 0.1% SDS prior to separation by SDS-PAGE on a 10% polyacrylamide gel. The separated membrane proteins were transferred to PVDF membrane (Millipore) by western blotting and incubated with rabbit-anti-iLR (1:2000) or rabbit-anti-LDLR antibodies (1:5000) as indicated for 2 hours, followed by 1 hour AP-GAR incubation. Hybridized AP-GAR was visualized by incubating the blot in TSM buffer, containing 100 mM Tris-HCl, 100 mM NaCl, 10 mM $MgAc_2$, 50 µg/ml p-nitro blue tetrazolium chloride (NBT; Boehringer Mannheim), 25 µg/ml 5-bromo-4-chloro-3-indoyl-phosphate p-toluidine (BCIP; Roche Diagnostics), pH 9.0.

Incubation of CHO cells with fluorescently-labeled ligands

LDL and HDLp (1 mg/ml) were fluorescently labeled in PBS with 50 µl/ml DiI in DMSO (3 µg/µl) at 37°C under continuous stirring for 16 hours and 3 hours, respectively. HDLp and RAP (1 mg/ml) were labeled with 20 µl/ml OG dissolved in DMSO (1 µg/µl) at room temperature under continuous stirring for 1 hour according to the manufacturer's instructions. Fluorescently-labeled lipoproteins were purified with Sephadex G-25 PD-10 columns (Amersham Pharmacia Biotech) to replace the PBS by incubation medium containing 10 mM HEPES, 50 mM NaCl, 10 mM KCl, 5 mM $CaCl_2$, 2 mM $MgSO_4$, pH 7.4. OG-RAP was dialyzed against incubation medium using standard cellulose membrane (Medicell International). For endocytic uptake, CHO cells were incubated with 10 µg/ml DiI-LDL, 25 µg/ml OG-HDLp, 3.6 µg/ml OG-RAP and 25 µg/ml TMR-Tf as indicated for 15 minutes at 37°C or 30 minutes at 18°C. Cells were rinsed in incubation medium and either directly fixed in 4% paraformaldehyde diluted in PBS for 30 minutes at room temperature, or chased in growth medium at 37°C for variable time periods. When indicated, nocodazole (5 µM) or monensin (25 µM) was added to the medium prior to, as well as during the chase.

Immunofluorescence

Fixed cells were washed twice with PBS buffer and permeabilized with PBS buffer supplemented with 1.0 mg/ml saponin (PBSS) for 5 minutes at room temperature. The cells were subsequently incubated with PBSS containing 50 mM glycin for 10 minutes and 5% BSA for 30 minutes at room temperature. The cells were blocked twice for 5 minutes with 0.1% cold water fish gelatin in PBSS (PBSSG) at room temperature and incubated with corresponding primary antibodies (1:500) for 1 hour at 37°C. After rinsing four times for 5 minutes with PBSSG at room temperature, the samples were processed for indirect immunofluorescence by incubation with Cy5-GAR for 30 minutes at 37°C and rinsed an additional four times with PBSSG.

Microscopy and image processing

Coverslips with fixed cells were mounted in Mowiol supplemented with anti-fade reagent (DABCO) and examined on a fluorescence Axioscop microscope (Zeiss) with a Hg HBO-50 lamp and a Plan-Neofluar 100×/1.30 oil lens. Using FITC/TRITC filters, digital images were acquired with a DXM 1200 digital camera and ACT-1 version 2.00 software (Nikon Corporation).

To image living cells, we mounted the coverslips in a temperature-controlled aluminium chamber and incubated the cells at 37°C in growth medium supplemented with 1 µl/ml 1 mM LT, where indicated. Confocal multicolour images of cells were acquired using

a Leica TCS-NT confocal laser scanning-system on an inverted microscope DMIRBE (Leica Microsystems) with a PL APO 40×/1.25-0.75 oil lens (Leica Microsystems) and an argon-krypton laser as excitation source. Emission of OG, excited with the 488 laser line, was detected using a 530/30 nm (RSP 580) bandpass filter. DiI, TMR and LT were excited with the 568 nm laser line and detected using a 600/30 nm (RSP 660) bandpass filter. The 647 nm laser line was used to excite Cy5 and emission was detected with a 665 nm longpass filter.

Images were processed using Scion Image beta version 4.0.2 (Scion Corporation) and PaintShop pro 7.00 (Jasc Software) software. SigmaPlot for Windows 4.00 (SPSS Inc) was used to generate surface fluorescence intensity mesh plots. To quantitate the relative intensity of fluorescently-labeled ligand in cells, the average brightness of pixels in manually defined areas covering the cells was determined using the Scion Image software. The digital data of more than 200 individual cells per data point were processed using Microsoft Excel 2000 (Microsoft Corporation) and plotted using the SigmaPlot software.

Incubation of CHO cells with ^{125}I-labeled ligands

HDLp was labeled with [125]I[iodine] using iodine monochloride according to McFarlane (McFarlane, 1958), resulting in a specific labeling activity of 85 and 236 cpm/ng HDLp. ^{125}I-RAP was prepared using chloramine-T according to Rodenburg et al. (Rodenburg et al., 1998), resulting in a specific labeling activity of ~45,000 cpm/ng protein. Two experiments were performed in duplicate, using wild-type CHO and CHO(iLR) cells that were cultured in 12-well plates and grown to ~70% confluency. The cells were incubated for 45 minutes at 37°C in incubation medium containing 25 µg/ml ^{125}I-HDLp or 83 ng/ml (2.1 nM) ^{125}I-RAP without monensin, followed by an additional 15 minutes in the presence of 25 µM monensin. The cells were placed on ice, washed twice with cold wash buffer, containing 150 mM NaCl, 50 mM Tris-HCl, 2% BSA, pH 7.4, and subsequently lysed and dissolved in 0.1 N NaOH. The radioactivity of samples was determined with a Tri Carb 2300 TR liquid scintillation analyzer (Packard) in Emulsifier Safe liquid scintillation fluid (Packard) and a maximal counting time of 10 minutes per sample. To determine the total cell protein per well, cells were washed thrice with 4°C HEPES buffer and incubated for 4 hours at 4°C in a lysis buffer, containing 50 mM Tris-HCl (pH 7.7), 150 mM NaCl, 0.1 mM benzamidine, 1 mg/ml leupeptin, 1 mg/ml aprotinin, and 1% NP40. Protein concentrations were determined using the colorimetric detergent compatible protein assay (Bio-Rad).

Results

Expression of iLR by stably transfected CHO cells

In order study the endocytic capacity of iLR in vitro, LDLR-deficient CHO [*ldlA* (Kingsley and Krieger, 1984)] cells that produce intracellular nonfunctional LDLR intermediates were stably transfected with the mammalian expression vector pcDNA3, harbouring the full-length iLR cDNA [*ldlA*(iLR) (Dantuma et al., 1999)]. Additionally, wild-type CHO cells were stably transfected with the same construct (CHO(iLR)) to be able to compare the intracellular pathways of internalized mammalian and insect lipoproteins, simultaneously. The expression of iLR by both transfected cell lines was analyzed using detergent cell extracts that were separated by SDS-PAGE under reducing and non-reducing conditions. The proteins were transferred to polyvinylidene fluoride (PVDF) membrane and immunoblotted with polyclonal anti-iLR rabbit antibody raised against the cytoplasmic tail of iLR. These western blots showed a similar iLR expression level of both transfected CHO
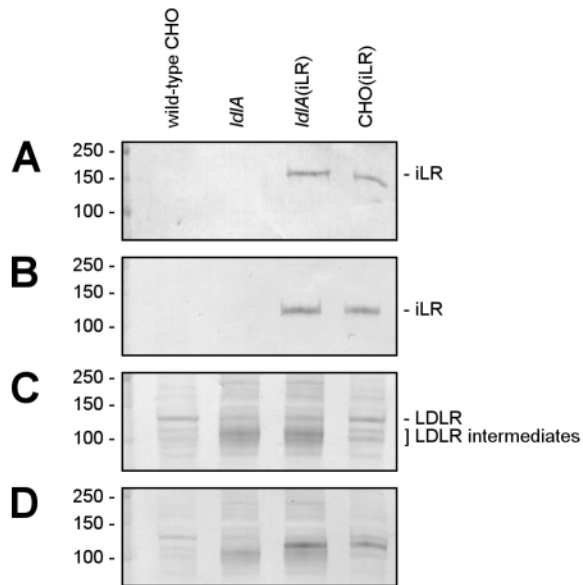
Fig. 1. iLR expression in CHO cell lines. Membrane proteins were
isolated from wild-type CHO, *ldlA*, *ldlA*(iLR) and CHO(iLR) cells as
described in Materials and Methods. Samples were either denatured
for 5 minutes at 95°C in Laemmli buffer (Laemmli, 1970) (A), or
dissolved in Laemmli buffer containing 0.1% SDS and directly
subjected to SDS-PAGE under non-reducing conditions (B,C,D).
Following transfer to PVDF membrane, iLR was detected with anti-
iLR antibody (A,B,D) and LDLR with anti-human LDLR antibody
(C,D). The molecular mass markers (kDa) are indicated on the left of
each panel.

Fig. 2. Receptor-mediated endocytic uptake of fluorescently-labeled
lipoproteins by CHO cells. CHO cells were incubated with
fluorescently-labeled lipoproteins in incubation medium for 15
minutes at 37°C, fixed with paraformaldehyde and mounted in
mowiol (A-F). Single cells were imaged using fluorescence
microscopy to visualize the accumulation of fluorescently-labeled
ligands in endocytic vesicles. CHO(iLR) (A) and *ldlA*(iLR) (B) cells
were incubated with DiI-LDL. HDLp labeled with DiI (C,D) or OG
(E,F) was used to incubate CHO(iLR) (C,E) and wild-type CHO
(D,F) cells. Uptake of fluorescently-labeled HDLp is reduced by an
excess of unlabeled HDLp. CHO(iLR) cells were also incubated for
15 minutes at 37°C (G) or 30 minutes at 18°C (H,I) in incubation
medium containing OG-HDLp in the absence (G,H) or presence (I)
of a tenfold excess of unlabeled HDLp. Bars, 20 µm.

cell lines (Fig. 1A,B). Under reducing conditions (Fig. 1A), the
apparent molecular mass of iLR increased from ~120 kDa (Fig.
1B, non-reducing conditions) to ~150 kDa (Fig. 1A, reducing
conditions), which is consistent with the reduction of multiple
disulfide bonds present in the cysteine class A repeats and
the EGF precursor homology domain. Moreover, the results
demonstrate that iLR is expressed as a receptor with a
molecular weight of ~150 kDa (Fig. 1A, reducing conditions),
which is higher than the predicted 98 kDa (Dantuma et al.,
1999). This suggests that the receptor is glycosylated, like
all the other members of the LDLR family (Russell et al.,
1984). The endogenous LDLR expression of CHO cells was
unaffected by transfection with iLR cDNA, as assessed from
western blot analysis using the polyclonal anti-LDLR rabbit
antibody raised against the extracellular domain of LDLR (Fig.
1C,D).

iLR mediates uptake of HDLp and human RAP in stably transfected CHO cells

To investigate the functional ligand-binding specificity of
iLR and LDLR, iLR-transfected cells were incubated with
fluorescently-labeled ligands in a buffer that was supplemented
with HEPES (i.e. incubation medium) to retard the transit of
internalized ligands at the early endosomal stage (Sullivan
et al., 1987). Upon 15 minutes of incubation at 37°C with
DiI-labeled human LDL (DiI-LDL), numerous cytoplasmic
vesicles distributed throughout CHO(iLR) cells could be
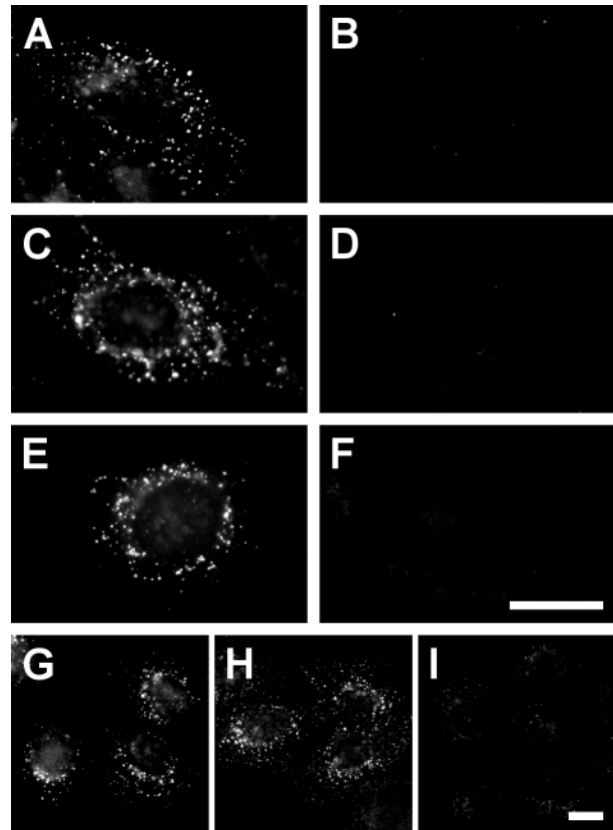observed (Fig. 2A). Such a punctate staining pattern, indicative

for receptor-mediated endocytosis, was absent in *ldlA*(iLR)
cells (Fig. 2B). This indicates that LDL uptake is exclusively
accomplished by the endogenous LDLR, and not a result of
aspecific endocytosis via iLR. A comparable particulate pattern
was observed in iLR-transfected cells incubated with DiI-
labeled HDLp (DiI-HDLp) (Fig. 2C), however, not in non-
transfected cells (Fig. 2D). DiI is a fluorescent lipid homologue
that incorporates in the lipid moiety of lipoproteins. To confirm
the concomitant endocytic uptake of the protein component of
the lipoprotein, HDLp was labeled covalently with the amine-
reactive fluorescent probe Oregon Green (OG). Analogous
incubation experiments with OG-labeled HDLp (OG-HDLp)
led to a similar endocytic uptake as could be visualized by DiI-
HDLp (Fig. 2E,F). These data suggest that the lipid uptake
mediated by iLR is a result of HDLp internalization rather
than a selective lipid-transfer mechanism occuring at the
cell surface. To verify that the internalized lipoproteins are

localized in endosomes after a 15 minutes incubation period at 37°C, the uptake experiments were repeated for 30 minutes at 18°C. Intracellular distribution of endocytosed ligands stagnates at a temperature of 18°C or below, preventing lysosomal degradation of ligands and recycling of receptors (Sullivan et al., 1987). The endocytic vesicle patterns of CHO(iLR) cells incubated at either temperature were indistinguishable (Fig. 2G,H), which strongly suggests that HDLp is transferred to sorting endosomes after receptor-mediated endocytosis. Uptake of fluorescently-labeled HDLp could be reduced with an equimolar concentration, and almost completely inhibited with a tenfold excess of unlabeled HDLp (Fig. 2I). This indicates that labeled and unlabeled HDLp compete for the same binding site. Therefore, it is most unlikely that the interaction between HDLp and iLR is altered by the covalently-bound OG label. From these experiments, we conclude that LDL uptake is restricted to endogenous LDLR-expressing cells and that HDLp uptake is exclusively mediated by iLR.

RAP has been shown to inhibit the binding of lipoproteins to LDLR family members, such as LDLR-related protein (LRP), very low-density lipoprotein receptor (VLDLR) and megalin (Herz et al., 1991; Kounnas et al., 1992; Battey et al., 1994), but has only weak affinity for LDLR itself (Medh et al., 1995). RAP serves as a molecular chaperone to assist the folding of several LDLR family members and prevents premature ligand interaction in the endoplasmic reticulum (Bu and Schwartz, 1998; Bu and Marzolo, 2000). As expected, when CHO(iLR) cells were incubated with DiI-LDL and an equimolar concentration of human RAP, endocytosis of LDL was not significantly reduced (Fig. 3A). However, endocytic uptake of HDLp could be completely prevented by an equimolar concentration of RAP (Fig. 3B). Inhibition of HDLp endocytosis by RAP indicates that iLR binds HDLp in the prevalent lipoprotein-binding manner, namely via its cysteine-rich ligand-binding domain (Dantuma et al., 1999). Additionally, the observation that a 1:1 ratio of RAP to OG-
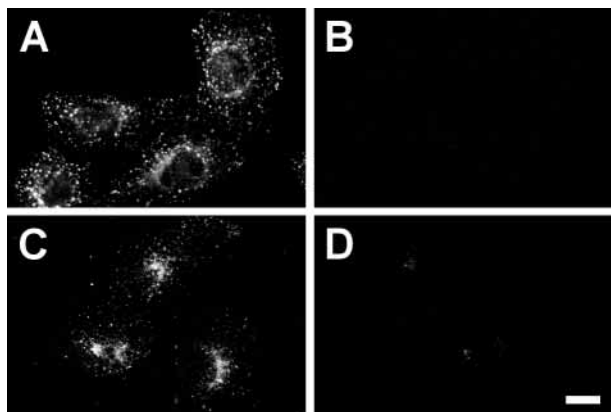
HDLp is sufficient to completely inhibit HDLp endocytosis suggests that, in comparison to HDLp, RAP has a higher affinity for iLR. Moreover, these data suggest that RAP is a ligand of iLR and, thus, could also be internalized by the insect receptor. To obtain evidence for this latter issue, we incubated CHO cells with OG-labeled RAP (OG-RAP) for 30 minutes at 18°C which resulted in a perinuclear vesicle distribution (Fig. 3C). Although the staining pattern appeared different from that observed in CHO(iLR) cells incubated with HDLp, endocytic uptake of RAP was clearly evident. Minor amounts of RAP could also be detected in endocytic vesicles of wild-type CHO cells (Fig. 3D), which is likely due to the expression of endogenous LRP and VLDLR. However, the fluorescence intensity of these vesicles was much lower in comparison to iLR-transfected cells, thus the majority of intracellular RAP in CHO(iLR) cells is endocytosed by iLR. The observation that, in addition to HDLp, RAP is also a ligand of iLR is in excellent agreement with iLR being an LDLR family member.

Mammalian and insect lipoproteins follow distinct intracellular routes

Receptor-bound LDL is rapidly delivered to sorting endosomes upon endocytosis by mammalian cells (Ghosh et al., 1994; Mellman, 1996; Mukherjee et al., 1997). The results of the incubation experiments at 18°C (Fig. 2H) suggest that HDLp and LDL are internalized and transferred to the same vesicles. To investigate whether HDLp accumulates in these tubulo vesicular endosomes, CHO(iLR) cells were incubated at 18°C with OG-HDLp in incubation medium supplemented with DiI-LDL. There was significant colocalization of HDLp (Fig. 4A) with LDL-containing endocytic vesicles (Fig. 4B,C) that were distributed throughout the cell, which supports the assumption that HDLp accumulates in sorting endosomes after endocytic uptake.

In sorting endosomes, LDL dissociates from LDLR due to mild luminal acidification after which the ligand is degraded in lysosomes. The receptor, however, is transported back to the cell surface via the ERC for additional uptake of extracellular LDL (Mellman, 1996; Mukherjee et al., 1997). By observing living cells with confocal laser scanning microscopy, we were able to visualize the sorting of mammalian and insect lipoproteins simultaneously, directly after endocytic uptake. CHO(iLR) cells were preincubated with OG-HDLp and DiI-LDL for 15 minutes at 37°C and subjected to a chase in growth medium without fluorescently-labeled ligands (chase medium) for an additional 30 minutes at 37°C. Within 10 minutes, a large amount of HDLp concentrated in the juxtanuclear area (Fig. 4D,E) in which LDL was almost completely absent (Fig. 4F,G). To investigate whether these vesicles were late endosomes or lysosomes, the membrane permeable probe, LysoTracker Yellow (LT), a weakly basic amine that selectively accumulates in cellular compartments with low luminal pH [i.e. lysosomes (Griffiths et al., 1988)], was added to the chase medium (Fig. 4H,I). As shown in Fig. 4J, there was almost no colocalization of HDLp with LT, and in areas where there was apparent overlap, the size and shape of the structures appeared different (Fig. 4K-M). This result implies that HDLp is not destined to be degraded via the classic LDL pathway. Together, these results confirm that, in contrast to LDL, internalized HDLp is not destined for lysosomal degradation.

Fig. 3. LDL endocytosis by CHO(iLR) cells is not significantly reduced by an equimolar concentration of RAP; however, endocytic uptake of HDLp is completely inhibited. CHO(iLR) cells were incubated for 30 minutes at 18°C with DiI-LDL (A) or OG-HDLp (B) in the presence of an equimolar concentration of unlabeled RAP. RAP is internalized by iLR-expressing CHO cells. CHO(iLR) (C) and wild-type CHO (D) cells were incubated with OG-RAP for 30 minutes at 18°C. Bar, 10 μm.

Fig. 4. HDLp colocalizes with LDL in early endocytic vesicles. CHO(iLR) cells were allowed to simultaneously internalize OG-HDLp (A) and DiI-LDL (B) in incubation medium for 30 minutes at 18°C. Fixed cells were analyzed using confocal laser microscopy to visualize the colocalization of the ligands in endosomes by overlaying the two images (C). Overlapping fluorescently labeled endosomes stain yellow after merging the layers. The HDLp-positive juxtanuclear compartment is depleted of LDL. CHO(iLR) cells were simultaneously preincubated with OG-HDLp and DiI-LDL. After the preincubation, the cells were transferred to an aluminium chamber and incubated in chase medium at 37°C. At 10 minutes, large amounts of HDLp concentrated in the juxtanuclear region (D), whereas LDL remained spatially distributed throughout the entire cell interior (F). Within a defined area (squares in D and F), the relative fluorescent intensity of the juxtanuclear-positioned structure was plotted on a relative scale (from 0 to 255, indicated by the vertical bar) for OG-HDLp (E) and DiI-LDL (G). Internalized HDLp accumulates in a non-lysosomal juxtanuclear compartment. CHO cells stably expressing iLR were preincubated with OG-HDLp, rinsed in HEPES buffer and mounted in an aluminium chamber. The cells were subsequently incubated at 37°C in chase medium that was supplemented with LT. Images were generated with multicolour imaging, using confocal laser microscopy to spatially visualize internalized HDLp and LT, simultaneously, in living cells. After a chase of 15 minutes, OG-HDLp-positive endocytic vesicles were highly concentrated in the juxtanuclear region (H), which was depleted of LT (I). Partial colocalization with LT was visualized by merging the two images (J). To enhance the visibility of the spatial distribution of HDLp and LT, a bright-field image of the observed cells was overlayed with fluorescent images. Additionally, detailed images of a single juxtanuclear structure were taken to visualize the minimal colocalization (K,L,M). Intracellular transport of ligands by iLR is microtubule-dependent. CHO(iLR) cells were preincubated with fluorescently-labeled ligand in the presence of 5 μM nocodazole. The cells were subsequently incubated for an additional 30 minutes at 37°C in chase medium supplemented with 5 μM nocodazole. Fixed cells were observed with confocal laser microscopy and showed a peripheral localization of vesicles that contained LDL (N), HDLp (O) or RAP (P). Bars, 20 μm.
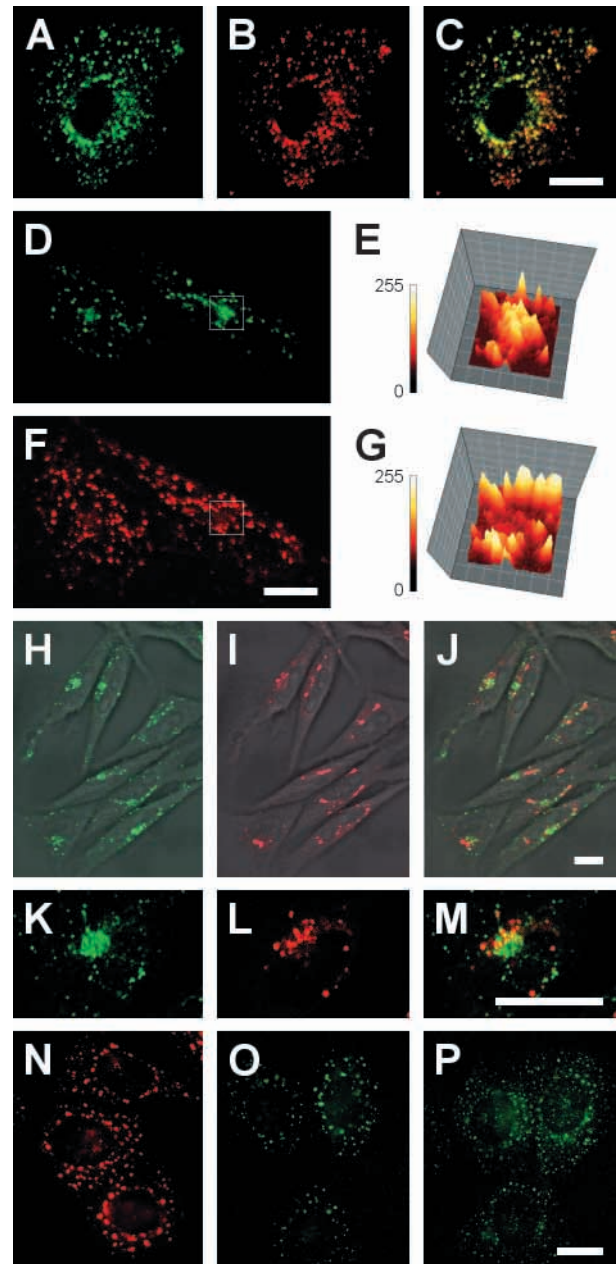
The microtubule-depolymerising agent nocodazole was used to investigate whether this perinuclear targeting was microtubule dependent. Depolymerization of microtubules has little effect on endocytosis, however, microtubule-dependent transport of internalized material is inhibited (Jin and Snider, 1993). Incubation of CHO(iLR) cells with DiI-LDL and OG-HDLp in the presence of 5 μM nocodazole followed by a chase for 30 minutes with an equal concentration of nocodazole resulted in the formation of enlarged LDL-labeled vesicles that were localized peripherally in the cells (Fig. 4N). A similar distribution of endocytic vesicles was observed when HDLp or RAP was used (Fig. 4O,P, respectively). Although HDLp- and RAP-containing vesicles appeared smaller in size and their fluorescence intensity less in comparison to LDL-containing vesicles, these data indicate that transit of iLR-bound ligands (i.e. HDLp and RAP) is microtubule dependent.

HDLp and RAP are transported to the ERC by iLR

To determine whether HDLp is translocated to the juxtanuclear localized ERC, we used Tf which converges in the ERC after endocytic uptake due to the durable association with TfR (Yamashiro et al., 1984; Mayor et al., 1993). CHO(iLR)

cells that were incubated with OG-HDLp and tetramethyl-rhodamine-labeled Tf (TMR-Tf), and subjected to a chase, show that HDLp is translocated to the ERC within 10 minutes (Fig. 5, left panel). Despite a small portion of individual vesicles that remained dispersed throughout the cell, the majority of HDLp colocalized with Tf in the ERC (Fig. 5, middle and right panel) from where molecules eventually exit the cell (Yamashiro et al., 1984). However, the gathering of HDLp in the ERC appeared slightly slower in comparison to the rapid transport of Tf, which is most likely the result of different sorting rates.

Additional evidence for the transport of HDLp to the ERC was obtained from experiments with monensin, a carboxylic ionophore which disrupts the route of recycling receptors (e.g. LDLR and TfR) by preventing the receptors from returning to the cell surface and thereby causing them to reside within the
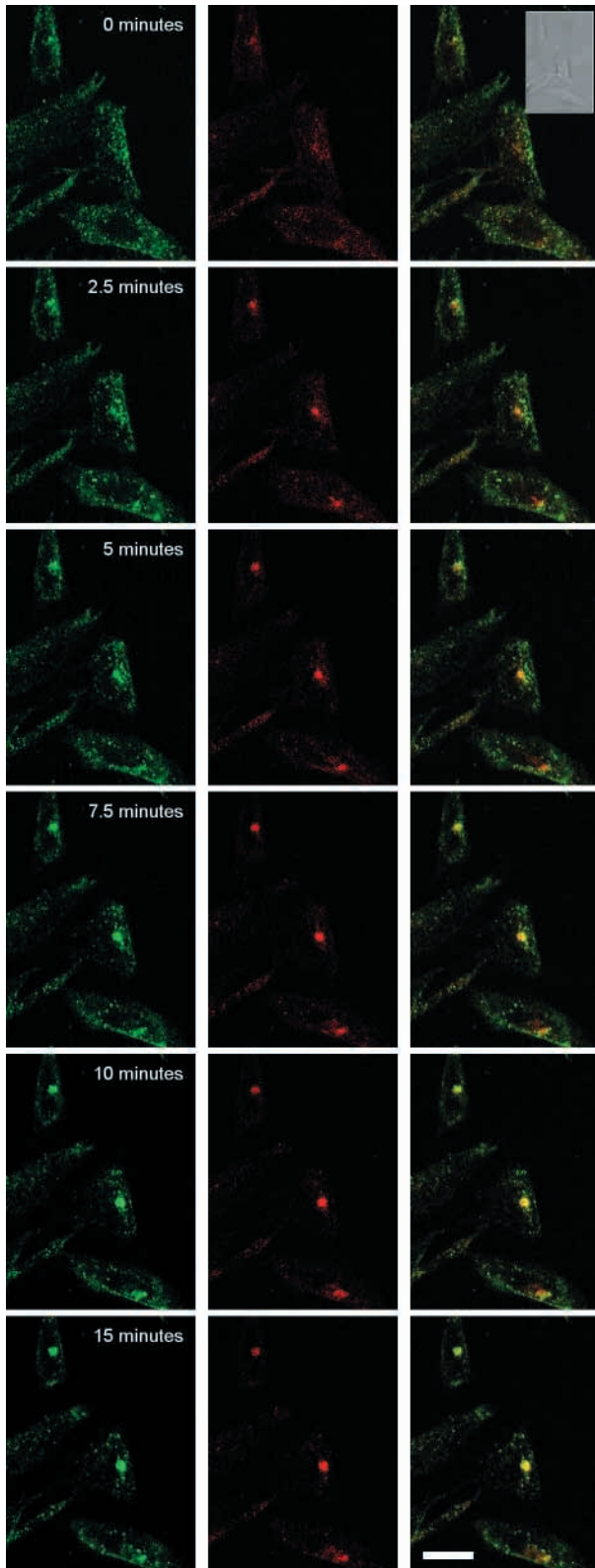
Fig. 5. HDLp colocalizes with internalized Tf in the ERC. Directly after preincubation for 20 minutes at 18°C with OG-HDLp and TMR-Tf, iLR-transfected CHO cells were rinsed in HEPES buffer and mounted in an aluminium chamber. The living cells were observed at 37°C in chase medium and imaged using confocal laser scanning microscopy. Digital multicolour images of OG-HDLp (left panel) and TMR-Tf (middle panel) were taken at defined time points as indicated in the left panel. Colocalization was visualized by merging the two images of the same time point (right panel). The insert in the upper right panel shows a bright-field image of the observed cells directly after preincubation. Bar, 20 μm.

significantly affect lysosomal targeting of LDL (Fig. 6A), however, HDLp accumulated in the juxtanuclear area (Fig. 6B). OG fluorescence observed in the ERC represents either undegraded OG-HDLp or OG released from degraded OG-HDLp. To confirm the concomitant transport of the non-exchangeable apolipoprotein matrix of HDLp with the fluorescent label OG to the ERC, we used antibodies against apoLp-I and -II to immunolocalize the proteins. Cells were fixed after preincubation with OG-HDLp and a chase of 30 minutes in the presence of monensin. The cells were subsequently incubated with anti-apoLp-I or -II rabbit antibodies (Schulz et al., 1987) which were visualized with a Cy5-labeled goat-anti-rabbit second antibody. Both apoLp-I (Fig. 6C) and apoLp-II (Fig. 6D) were predominantly localized in the ERC and show significant overlap with OG (Fig. 6E-H). We interpret these data to indicate that the complete non-exchangeable protein matrix of HDLp, comprising apoLp-I and -II, is transported to the ERC.

Above we showed that iLR is capable of binding and internalizing human RAP (Fig. 3C). To investigate whether endocytosed RAP is also transported to the ERC, we repeated the incubation experiments with monensin using RAP. Subjecting CHO(iLR) cells to a chase after preincubation with OG-RAP in the presence of monensin resulted in the convergence of RAP in a single spot near the nucleus (Fig. 7A). When TMR-Tf was used in combination with OG-RAP, there was significant colocalization of RAP and Tf in the ERC (Fig. 7B-D). This implies that the pathways of ligands that are internalized by iLR are determined by the intracellular route of the receptor. To visualize the intracellular localization of iLR, we used anti-iLR antibody and the Cy5-labeled second antibody to detect iLR in fixed CHO(iLR) cells. Preincubation of these cells with OG-HDLp followed by a chase in medium containing monensin shows that the ligand is localized in the ERC (Fig. 7E), the organelle in which iLR is also located (Fig. 7F,G). Even in the absence of ligand or monensin, the receptor was predominantly present in the ERC (Fig. 7H), suggesting constitutive recycling of iLR without antecedent ligand binding as observed for LDLR (Anderson et al., 1982; Brown et al., 1982) and TfR (Stein and Sussman, 1986).

To quantify iLR-specific uptake, and subsequent transfer to the ERC of HDLp and RAP, we incubated wild-type CHO and CHO(iLR) cells with ^{125}I-labeled HDLp and RAP in the presence of monensin. Cells were preincubated with the ^{125}I-labeled ligands for 45 minutes at 37°C without monensin, followed by a shorter second incubation of 15 minutes at 37°C with the ^{125}I-labeled ligands in the presence of 25 μM monensin. These experiments revealed an iLR-mediated HDLp uptake of 112 ng/mg cell protein (means of two duplo

ERC (Basu et al., 1981; Stein et al., 1984). A concentration of 25 μM monensin appeared sufficient to interrupt receptor recycling and trap internalized receptors of CHO(iLR) cells that were preincubated with DiI-LDL or OG-HDLp, and chased for an additional 30 minutes. Monensin did not

experiments, s.e.m.±27), which corresponds to ~350 pmol/mg cell protein. iLR-specific uptake of RAP was also determined and appeared to be 61.3 ng/mg cell protein (mean of duplo experiment, s.e.m.±0.44), the equivalent of ~1570 pmol/mg

Fig. 6. Internalized HDLp is trapped intracellularly by monensin. CHO(iLR) cells were incubated with fluorescently-labeled ligands in the presence of 25 µM monensin for 30 minutes at 18°C. The cells were subsequently chased for 30 minutes at 37°C with an equal concentration of monensin and mounted in mowiol after fixation. LDL was scattered throughout the cell in vesicles (A); however, HDLp was predominantly located in the juxtanuclear area (B). The non-exchangeable protein matrix of HDLp is transported to the ERC. CHO(iLR) cells were allowed to take up OG-HDLp for 15 minutes at 37°C in the presence of 25 µM monensin. After a chase of 30 minutes with an equal concentration of monensin, the cells were washed and labeled with antibodies against apoLp-I and -II, which were visualized with a Cy5-labeled second antibody. The fluorescent label OG that represents intracellular HDLp (C,D) colocalized with apoLp-I (E) and -II (F) in the juxtanuclear area (G,H). Bars, 10 µm.

cell protein. This ~4.5-fold higher uptake of RAP in comparison to HDLp is in good agreement with the observation that a 1:1 ratio of RAP to OG-HDLp is sufficient to completely inhibit HDLp endocytosis (Fig. 3B). Moreover, it supports the relatively higher affinity of RAP for iLR in comparison to that of HDLp, as suggested above.
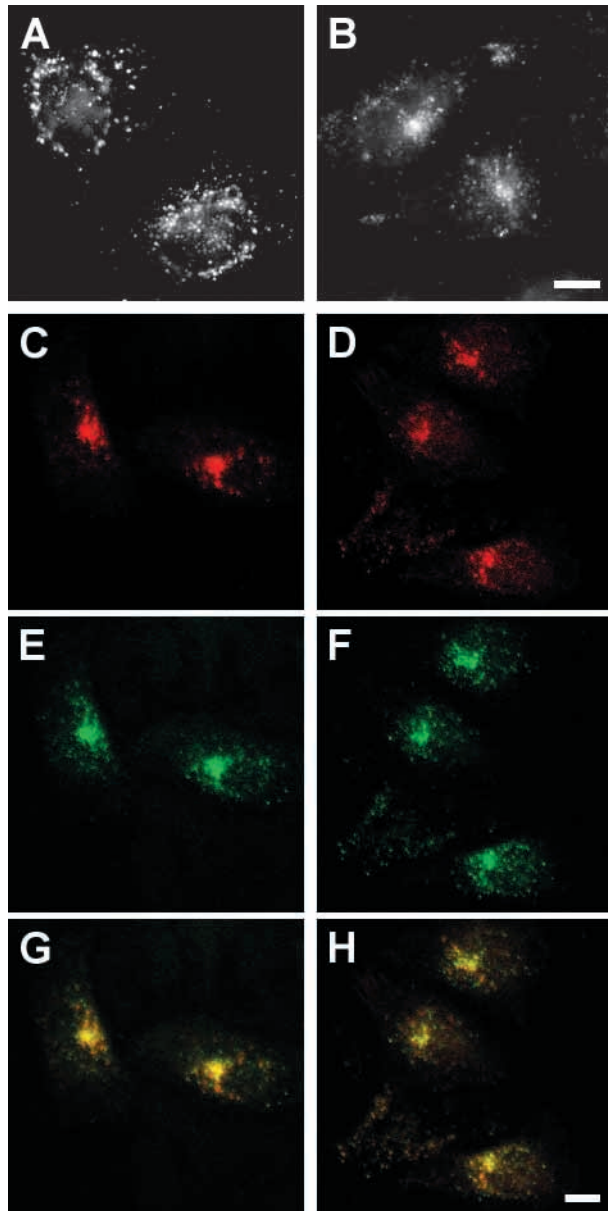
HDLp is re-secreted from CHO(iLR) cells with a $t_{1/2}$ of ~13 minutes

Convergence of HDLp in the ERC implies that the ligand is eventually re-secreted into the medium (Yamashiro et al., 1984). Quantitative fluorescence microscopy was used to determine the exit rate of intracellular HDLp and LDL. CHO(iLR) cells were analyzed after a preincubation of OG-HDLp and DiI-LDL to label the endocytic pathway. Shortly after initiating the chase, the clearly visible ERC predominantly contained HDLp, in which no significant amount of LDL could be detected (Fig. 8A). In contrast, the spatially distributed vesicles that were numerously present contained mainly LDL, some of which harbouring only a minor amount of HDLp. During the chase, the relative fluorescent intensity of OG-HDLp in the ERC decreased dramatically compared to that of the individual, LDL-containing vesicles (Fig. 8B-F). Total intracellular fluorescence of OG-HDLp and DiI-LDL in cells that were fixed after a chase at defined time points were determined (Fig. 8G). The plotted data show that the relative fluorescence of intracellular OG-HDLp rapidly decreases, whereas that of DiI-LDL remains constant during a 60 minutes chase. From these observations, we conclude that HDLp exits the cells with a $t_{1/2}$ of ~13 minutes, which is in good agreement with that of Tf (Mayor et al., 1993; Ghosh et al., 1994). The clearance of intracellular HDLp strongly suggests that HDLp is re-secreted after passage through the ERC.

Taken together, all the results indicate that HDLp uptake is specifically mediated by iLR. In addition to insect lipoprotein, iLR is capable of binding and internalizing human RAP. In contrast to LDL, which ends up in lysosomes, ligands that are internalized by iLR are not destined for lysosomal degradation. As a result of the intracellular pathway of the receptor, iLR-coupled ligands follow a transferrin-like intracellular recycling route.

Discussion

A generally accepted property of LDLR family members is their ability to endocytose ligands and transport them to sorting endosomes. Due to the low lumenal pH, the internalized ligands are released from their receptors and transported to lysosomes for degradation. The receptors are transported back to the cell surface via the ERC and thereby escape lysosomal hydrolysis. In vertebrates, LDLR-mediated endocytosis of LDL is essential for plasma cholesterol homeostasis. In consistence with the expected fate of lipoproteins, LDL is degraded in lysosomes and resulting lipid components are released into the cytoplasm (Brown and Goldstein, 1986). Here we report a novel intracellular distribution and fate of an apoB homologue-containing lipoprotein, HDLp, which escapes its expected degradation in iLR-transfected CHO cells. Recycling of exchangeable apolipoproteins upon receptor-mediated
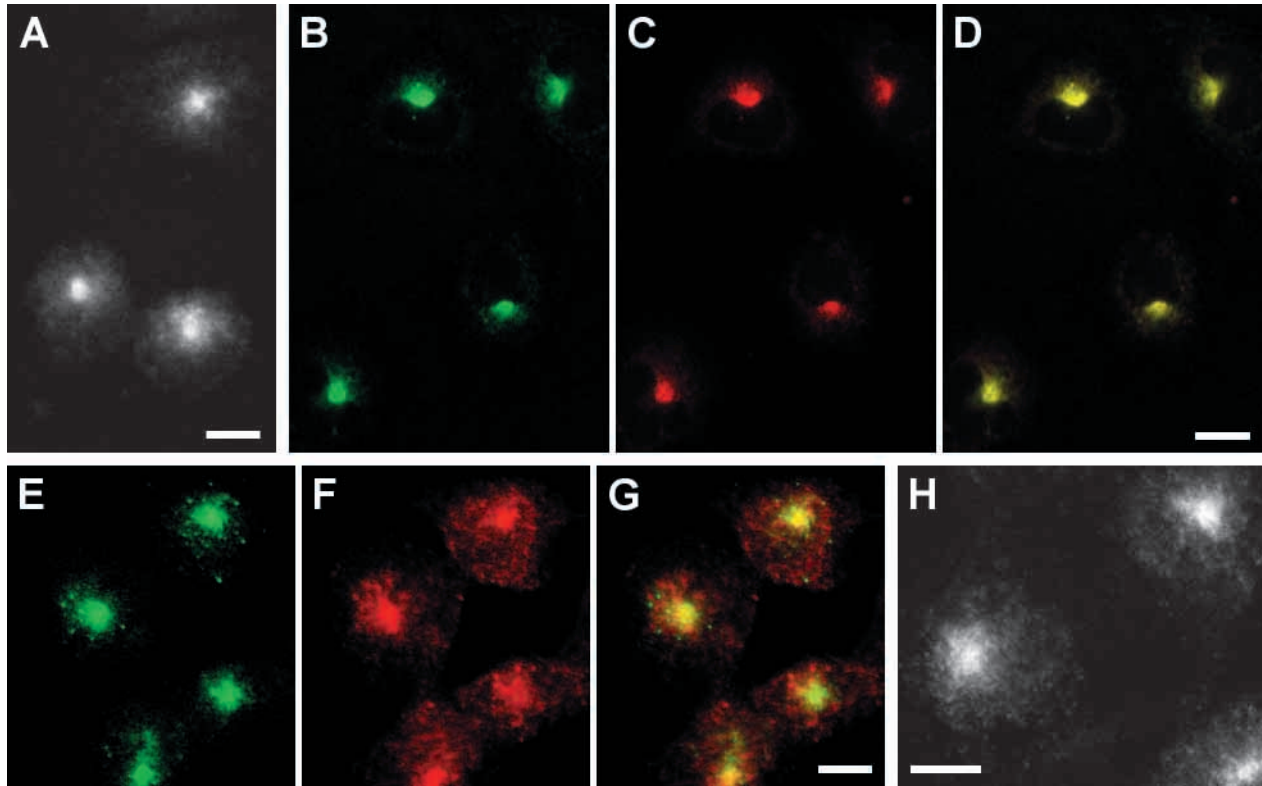
Fig. 7. Internalized RAP accumulates in the juxtanuclear area. CHO(iLR) cells preincubated with OG-RAP and chased for 30 minutes at 37°C in the presence of 25 μM monensin were fixed and mounted in mowiol. The cells were observed with fluorescence microscopy to visualize RAP that was predominantly located in the juxtanuclear region (A). RAP follows a transferrin-like intracellular pathway. CHO(iLR) cells were simultaneously preincubated with OG-RAP and TMR-Tf and chased for 30 minutes in the presence of 25 μM monensin. Digital images of fixed cells containing RAP (B) and Tf (C) were generated with laser scanning microscopy and the colocalization in the juxtanuclear area was visualized by merging the two images (D). HDLp colocalizes with iLR in the ERC. To determine the localization of iLR after preincubation with OG-HDLp and chase for 30 minutes in the presence of 25 μM monensin, CHO(iLR) cells were fixed and labeled with antibodies against iLR which were visualized with a Cy5-labeled second antibody. OG-HDLp (E) and iLR (F) show significant overlap in the ERC (G). iLR is also abundantly located in the ERC in the absence of ligand or monensin. CHO(iLR) cells were fixed after treatment with incubation medium for 15 minutes at 37°C and iLR was visualized as described above (H). Bars, 10 μm.

endocytosis is not unique [e.g. apolipoprotein C (Heeren et al., 1999); and E (Fazio et al., 1999; Rensen et al., 2000)]; however, the recycling of non-exchangeable apolipoprotein, such as apoB, has not yet been described to occur in mammalian cells. On the basis of the results presented in this study, we conclude that, despite the non-exchangeable protein matrix being the sole apolipoprotein compound of HDLp, the intracellular route of this lipoprotein deviates from the classic lysosome-directed pathway.

CHO cells that are transfected with iLR cDNA mediate endocytosis of HDLp, however, the ligand remains in complex with the receptor in sorting endosomes. Several LDLR family member mutants have been constructed to identify the responsible domains and investigate the biochemical mechanisms involved in ligand uncoupling due to an acidic pH (Davis et al., 1987; Mikhailenko et al., 1999). Here we present evidence for the first naturally occurring LDLR family member, the ligands of which remain coupled to iLR in sorting endosomes and are consequently transported to the ERC to be eventually re-secreted in a transferrin-like manner.

Re-secretion of HDLp after endocytosis is consistent with the role for HDLp as a reusable shuttle for selective lipid delivery. The major difference between insect and mammalian lipoproteins is the selective mechanism by which insect lipoproteins transfer their hydrophobic cargo. Dependent on the physiological situation, circulating HDLp particles serve as either DAG acceptors at the insect fat body during adult stage-restricted flight activity, or donors during dietary lipid storage in the fat body of larval and young adult insects (Van der Horst, 1990; Ryan and Van der Horst, 2000; Van der Horst et al., 2001; Van der Horst et al., 2002). In the latter case, endocytic uptake of HDLp seems to conflict with the selective unloading of lipids from HDLp to fat body cells without concurrent degradation of the ligand (Arrese et al., 2001). In experiments in which fat body tissue from young adult locusts was incubated with HDLp containing ^{3}H-labeled DAG and apolipoproteins, ^{3}H-DAG appeared to be taken up selectively without substantial concomitant accumulation of the radiolabeled apolipoproteins (Dantuma et al., 1997). Endocytosis of HDLp for lipid storage in fat body cells had earlier been postulated for the insect *Ashna cyanea* (Bauerfeind and Komnick, 1992). However, thus far, evidence for recycling of the ligand had not been described. Our observations with fluorescently-labeled HDLp strongly support that, despite

receptor-mediated internalization of the ligand, HDLp can be used as a reusable shuttle in both physiological conditions. Moreover, we provide preliminary evidence for the existence of a novel selective lipid-uptake mechanism mediated by an LDLR homologue that takes place intracellularly.

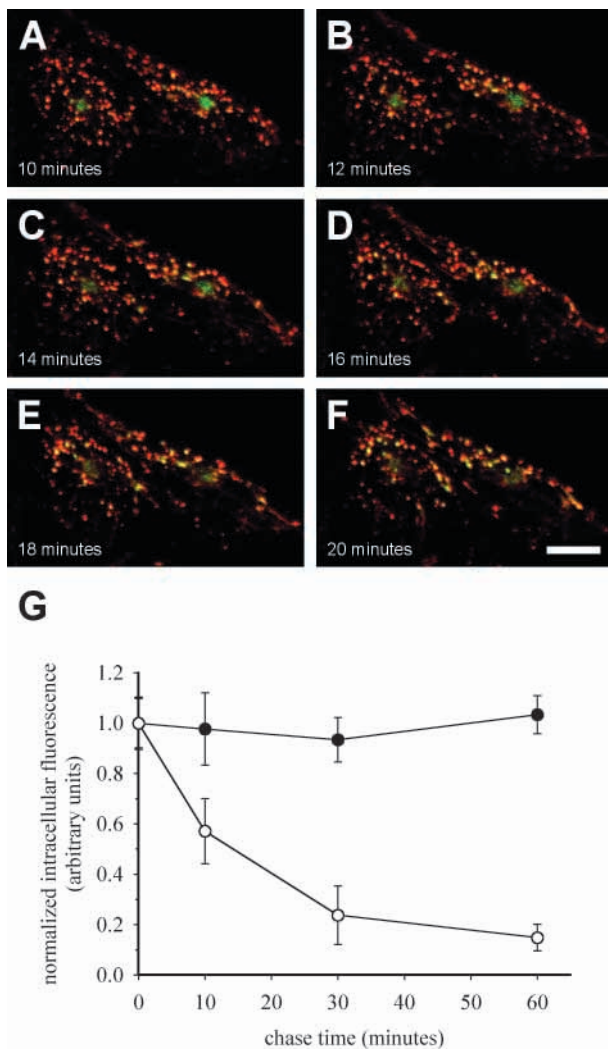Despite structural homology between LDL and HDLp at the

Fig. 8. HDLp exits CHO(iLR) cells with a t½ of ~13 minutes. Living CHO(iLR) cells, preincubated with DiI-LDL and OG-HDLp, were observed in an aluminium chamber with confocal laser microscopy during a chase for 20 minutes. Digital photos were collected 10 minutes after initiating the chase at 2 minute time intervals (A-F) to visualize the intracellular distribution of LDL (red) and HDLp (green). To quantify the re-secretion of internalized fluorescently-labeled lipoproteins, CHO(iLR) cells were fixed directly after preincubation with DiI-LDL (filled circles) or OG-HDLp (open circles), and after a chase for 10, 30 or 60 minutes (G). Images were recorded using confocal laser scanning microscopy and analyzed with Scion Image software. The data points are geometric means of the measured relative intensity of total cells. Of each time point, 10 to 17 images were taken with 4 to 33 cells per image, corresponding to more than 200 cells per data point. The mean values were normalized to the measurement directly after the preincubation. The data were processed with Microsoft Excel and plotted with SigmaPlot. Bar, 20 µm; values are means±s.e.m. of 10 or more digital images.

protein level, we have shown that iLR specifically internalizes the insect lipoprotein, whereas LDLR exclusively mediates uptake of LDL. In addition to HDLp, iLR shows a relatively high affinity for human RAP; a feature that is not shared by LDLR (Medh et al., 1995). However, all other members of the LDLR family have been observed to bind RAP with high affinity and internalize this ligand (Neels et al., 1998). The ability of iLR to bind human RAP is in line with the presence of a RAP homologous gene identified in the *Drosophila* genome (Adams et al., 2000).

Transition of internalized HDLp to the ERC is mediated by the membrane-spanning iLR in analogy to Tf recycling (Yamashiro et al., 1984). In contrast to the uncoupling of mammalian LDL from LDLR in sorting endosomes, HDLp remains attached to its receptor despite the decrease in lumenal pH. Endosome tubulation followed by iterative fractionation of membrane-anchored recycling receptors results in efficient receptor recycling by default (Dunn et al., 1989; Verges et al., 1999). Consequently, ligands that remain coupled to such receptors are recycled as well. Davis et al. showed that the EGF-precursor homology domain of LDLR is responsible for acid-dependent ligand dissociation (Davis et al., 1987). In addition, Mikhailenko et al. produced a VLDLR mutant of which the EGF-precursor homology domain was deleted (Mikhailenko et al., 1999). They demonstrated that, in contrast to wild-type VLDLR, RAP did not dissociate from the mutant receptor after internalization and was not degraded. By using RAP as well as HDLp, we show that iLR is capable of transporting physiologically unrelated ligands to the ERC, despite having a typical ligand-dissociating EGF-precursor homology domain. Our results combined with earlier observations using ^{3}H-labeled HDLp to incubate fat body cells indicate that iLR-mediated recycling of HDLp plays a physiologically relevant role in lipid storage (Dantuma et al., 1997). A selective lipid extration mechanism would significantly reduce degradation as well as energy-consuming synthesis of reusable HDLp.

Cellular uptake of HDLp and human RAP by iLR results in an intracellular distribution of both ligands that deviates from the classic lysosomal delivery of mammalian lipoproteins in CHO cells. These observations propose a novel mechanism for ligand-uptake by an LDLR family member that is present in insects. It has been suggested that specific mammalian tissues may selectively take up lipoprotein-bound components with LDLR homologous receptors (e.g. LRP), however, without endocytosis of the ligand (Vassiliou et al., 2001; Swarnakar et al., 2001). Additionally, alternative functions for LDLR that deviate from the classic lysosomal lipoprotein delivery could also depend on the developmental stage or type of tissue (Dehouck et al., 1997). Our model system using iLR and CHO cells provides a powerful tool to study the molecular basis for the intracellular distribution and fate of ligands that are internalized by LDL receptors, as well as the function of individual receptor domains. An important issue to be solved remains the understanding of the molecular basis for the difference in targeting behaviour of the mammalian and insect receptors. Although LDLR and iLR share a 57% sequence similarity, small differences in receptor domains might determine the fate of bound ligands. Whereas the ligand-binding domain of LDLR comprises seven cysteine-rich repeats, iLR has eight of these modules. The larger ligand-

binding domain could cause a more stable ligand-receptor interaction, preventing acid-induced uncoupling in the endosomal compartment that is mediated by the EGF-precursor homology domain. In addition, the twelve C-terminal amino acids of the cytoplasmic tail of LDLR are completely different compared to those of iLR. Moreover, the intracellular portion of iLR has an additional 10 amino acids. These residues could possibly interact with cytosolic components involved in processes that direct ligand distribution. Further analysis of insect lipoproteins and receptors, as well as the construction of hybrid receptors that are composed of (parts of) insect and mammalian receptors, will provide new insights into the understanding of molecular mechanisms that regulate lipoprotein binding and lipid uptake in mammals.

References

Adams, M. D., Celniker, S. E., Holt, R. A., Evans, C. A., Gocayne, J. D., Amanatides, P. G., Scherer, S. E., Li, P. W., Hoskins, R. A., Galle, R. F. et al. (2000). The genome sequence of *Drosophila melanogaster*. *Science* **287**, 2185-2195.

Anderson, R. G. W., Brown, M. S., Beisiegel, U. and Goldstein, J. L. (1982). Surface distribution and recycling of the low density lipoprotein receptor as visualized with antireceptor antibodies. *J. Cell Biol.* **93**, 523-531.

Arrese, E. L., Canavoso, L. E., Jouni, Z. E., Pennington, J. E., Tsuchida, K. and Wells, M. A. (2001). Lipid storage and mobilization in insects: current status and future directions. *Insect Biochem. Mol. Biol.* **31**, 7-17.

Babin, P. J., Bogerd, J., Kooiman, F. P., van Marrewijk, W. J. A. and van der Horst, D. J. (1999). Apolipophorin II/I, apolipoprotein B, vitellogenin, and microsomal triglyceride transfer protein genes are derived from a common ancestor. *J. Mol. Evol.* **49**, 150-160.

Basu, S. K., Goldstein, J. L., Anderson, R. G. and Brown, M. S. (1981). Monensin interrupts the recycling of low density lipoprotein receptors in human fibroblasts. *Cell* **24**, 493-502.

Battey, F., Gafvels, M. E., Fitzgerald, D. J., Argraves, W. S., Chappell, D. A., Straus, J. F., III and Strickland, D. K. (1994). The 39 kDa receptor-associated protein regulates ligand binding by the very low density lipoprotein receptor. *J. Biol. Chem.* **269**, 23268-23273.

Bauerfind, R. and Komnick, H. (1992). Immunocytochemical localization of lipophorin in the fat body of dragonfly larvae (*Aeshna cyanea*). *J. Insect Physiol.* **38**, 185-198.

Bogerd, J., Babin, P. J., Kooiman, F. P., Andre, M., Ballagny, C., van Marrewijk, W. J. A. and van der Horst, D. J. (2000). Molecular characterization and gene expression in the eye of the apolipophorin II/I precursor from Locusta migratoria. *J. Comp. Neurol.* **427**, 546-558.

Brown, M. S. and Goldstein, J. L. (1986). A receptor-mediated pathway for cholesterol homeostasis. *Science* **232**, 34-47.

Brown, M. S., Anderson, R. G., Basu, S. K. and Goldstein, J. L. (1982). Recycling of cell-surface receptors: observations from the LDL receptor system. *Cold Spring Harb. Symp. Quant. Biol.* **46**, 713-721.

Brown, M. S., Herz, J. and Goldstein, J. L. (1997). LDL-receptor structure. Calcium cages, acid baths and recycling receptors. *Nature* **388**, 629-630.

Bu, G. and Marzolo, M. P. (2000). Role of RAP in the biogenesis of lipoprotein receptors. *Trends Cardiovasc. Med.* **10**, 148-155.

Bu, G. and Schwartz, A. L. (1998). RAP, a novel type of ER chaperone. *Trends Cell Biol.* **8**, 272-275.

Dantuma, N. P., van Marrewijk, W. J. A., Wynne, H. J. and van der Horst,

D. J. (1996). Interaction of an insect lipoprotein with its binding site at the fat body. *J. Lipid Res.* **37**, 1345-1355.

Dantuma, N. P., Pijnenburg, M. A., Diederen, J. H. B. and van der Horst, D. J. (1997). Developmental down-regulation of receptor-mediated endocytosis of an insect lipoprotein. *J. Lipid Res.* **38**, 254-265.

Dantuma, N. P., Potters, M., de Winther, M. P., Tensen, C. P., Kooiman, F. P., Bogerd, J. and van der Horst, D. J. (1999). An insect homolog of the vertebrate very low density lipoprotein receptor mediates endocytosis of lipophorins. *J. Lipid Res.* **40**, 973-978.

Davis, C. G., Goldstein, J. L., Sudhof, T. C., Anderson, R. G., Russell, D. W. and Brown, M. S. (1987). Acid-dependent ligand dissociation and recycling of LDL receptor mediated by growth factor homology region. *Nature* **326**, 760-765.

Dehouck, B., Fenart, L., Dehouck, M. P., Pierce, A., Torpier, G. and Cecchelli, R. (1997). A new function for the LDL receptor: transcytosis of LDL across the blood-brain barrier. *J. Cell Biol.* **138**, 877-889.

Dunn, K. W. and Maxfield, F. R. (1992). Delivery of ligands from sorting endosomes to late endosomes occurs by maturation of sorting endosomes. *J. Cell Biol.* **117**, 301-310.

Dunn, K. W., McGraw, T. E. and Maxfield, F. R. (1989). Iterative fractionation of recycling receptors from lysosomally destined ligands in an early sorting endosome. *J. Cell Biol.* **109**, 3303-3314.

Fazio, S., Linton, M. F., Hasty, A. H. and Swift, L. L. (1999). Recycling of apolipoprotein E in mouse liver. *J. Biol. Chem.* **274**, 8247-8253.

Ghosh, R. N., Gelman, D. L. and Maxfield, F. R. (1994). Quantification of low density lipoprotein and transferrin endocytic sorting HEp2 cells using confocal microscopy. *J. Cell Sci.* **107**, 2177-2189.

Goldstein, J. L., Brown, M. S., Anderson, R. G. W., Russell, D. W. and Schneider, W. J. (1985). Receptor-mediated endocytosis: concepts emerging from the LDL receptor system. *Annu. Rev. Cell Biol.* **1**, 1-39.

Griffiths, G., Hoflack, B., Simons, K., Mellman, I. and Kornfeld, S. (1988). The mannose 6-phosphate receptor and the biogenesis of lysosomes. *Cell* **52**, 329-341.

Heeren, J., Weber, W. and Beisiegel, U. (1999). Intracellular processing of endocytosed triglyceride-rich lipoproteins comprises both recycling and degradation. *J. Cell Sci.* **112**, 349-359.

Herz, J., Goldstein, J. L., Strickland, D. K., Ho, Y. K. and Brown, M. S. (1991). 39-kDa protein modulates binding of ligands to low density lipoprotein receptor-related protein/α2-macroglobulin receptor. *J. Biol. Chem.* **266**, 21232-21238.

Hussain, M. M., Strickland, D. K. and Bakillah, A. (1999). The mammalian low-density lipoprotein receptor family. *Annu. Rev. Nutr.* **19**, 141-172.

Jin, M. and Snider, M. D. (1993). Role of microtubules in transferrin receptor transport from the cell surface to endosomes and the Golgi complex. *J. Biol. Chem.* **268**, 18390-18397.

Kingsley, D. M. and Krieger, M. (1984). Receptor-mediated endocytosis of low density lipoprotein: somatic cell mutants define multiple genes required for expression of surface-receptor activity. *Proc. Natl. Acad. Sci. USA* **81**, 5454-5458.

Kounnas, M. Z., Church, F. C., Argraves, W. S. and Strickland, D. K. (1992). The 39-kDa receptor-associated protein interacts with two members of the low density lipoprotein receptor family, α2-macroglobulin receptor and glycoprotein 330. *J. Biol. Chem.* **267**, 21162-21166.

Laemmli, U. K. (1970). Cleavage of structural proteins during the assembly of the head of bacteriophage T4. *Nature* **227**, 680-685.

Mann, C. J., Anderson, T. A., Read, J., Chester, S. A., Harrison, G. B., Kochl, S., Ritchie, P. J., Bradbury, P., Hussain, F. S., Amey, J. et al. (1999). The structure of vitellogenin provides a molecular model for the assembly and secretion of atherogenic lipoproteins. *J. Mol. Biol.* **285**, 391-408.

Mayor, S., Presley, J. F. and Maxfield, F. R. (1993). Sorting of membrane components from endosomes and subsequent recycling to the cell surface occurs by a bulk flow process. *J. Cell Biol.* **121**, 1257-1269.

McFarlane, A. S. (1958). Efficient trace-labelling of proteins with iodine. *Nature* **82**, 53.

Medh, J. D., Fry, G. L., Bowen, S. L., Pladet, M. W., Strickland, D. K. and Chappell, D. A. (1995). The 39-kDa receptor-associated protein modulates lipoprotein catabolism by binding to LDL receptors. *J. Biol. Chem.* **270**, 536-540.

Mellman, I. (1996). Endocytosis and molecular sorting. *Annu. Rev. Cell Dev. Biol.* **12**, 575-625.

Mikhailenko, I., Considine, W., Argraves, K. M., Loukinov, D., Hyman, B. T. and Strickland, D. K. (1999). Functional domains of the very low density lipoprotein receptor: molecular analysis of ligand binding and acid-dependent ligand dissociation mechanisms. *J. Cell Sci.* **112**, 3269-3281.

Mukherjee, S., Ghosh, R. N. and Maxfield, F. R. (1997). Endocytosis. *Physiol. Rev.* **77**, 759-803.

Neels, J. G., Horn, I. R., van den Berg, B. M. M., Pannekoek, H. and van Zonneveld, A. J. (1998). Ligand-receptor interactions of the low density lipoprotein receptor-related protein, a multi-ligand endocytic receptor. *Fibrinolysis Proteolysis* **12**, 219-240.

Redgrave, T. G., Roberts, D. C. and West, C. E. (1975). Separation of plasma lipoproteins by density-gradient ultracentrifugation. *Anal. Biochem.* **65**, 42-49.

Rensen, P. C. N., Jong, M. C., van Vark, L. C., van der Boom, H., Hendriks, W. L., van Berkel, T. J. C., Biessen, E. A. L. and Havekes, L. M. (2000). Apolipoprotein E is resistant to intracellular degradation in vitro and in vivo. Evidence for retroendocytosis. *J. Biol. Chem.* **275**, 8564-8571.

Rodenburg, K. W., Kjøller, L., Petersen, H. H. and Andreasen, P. A. (1998). Binding of urokinase-type plasminogen activator/plasminogen activator inhibitor-1 complex to endocytosis receptors α_2-macroglobulin receptor/low density lipoprotein receptor-related protein and very low density lipoprotein receptor involves basic residues in the inhibitor. *Biochem. J.* **329**, 55-63.

Russell, D. W., Schneider, W. J., Yamamoto, T., Luskey, K. L., Brown, M. S. and Goldstein, J. L. (1984). Domain map of the LDL receptor: sequence homology with the epidermal growth factor precursor. *Cell* **37**, 577-585.

Ryan, R. O. and van der Horst, D. J. (2000). Lipid transport biochemistry and its role in energy production. *Annu. Rev. Entomol.* **45**, 233-568.

Schulz, T. K. F., van der Horst, D. J., Amesz, H., Voorma, H. O. and Beenakkers, A. M. T. (1987). Monoclonal antibodies specific for apoproteins of lipophorins from the migratory locust. *Arch. Insect Pysiol. Biochem.* **6**, 97-107.

Segrest, J. P., Jones, M. K., de Loof, H. and Dashti, N. (2001). Structure of apolipoprotein B-100 in low density lipoproteins. *J. Lipid Res.* **42**, 1346-1367.

Shelness, G. S. and Sellers, J. A. (2001). Very-low-density lipoprotein assembly and secretion. *Curr. Opin. Lipidol.* **12**, 151-157.

Soulages, J. L. and Wells, M. A. (1994). Lipophorin: the structure of an insect lipoprotein and its role in lipid transport in insects. *Adv. Protein Chem.* **45**, 371-415.

Stein, B. S. and Sussman, H. H. (1986). Demonstration of two distinct transferrin receptor recycling pathways and transferrin-independent receptor internalization in K562 cells. *J. Biol. Chem.* **261**, 10319-10331.

Stein, B. S., Bensch, K. G. and Sussman, H. H. (1984). Complete inhibition of transferrin recycling by monensin in K562 cells. *J. Biol. Chem.* **259**, 14762-14772.

Sullivan, P. C., Ferris, A. L. and Storrie, B. (1987). Effects of temperature, pH elevators, and energy production inhibitors on horseradish peroxidase transport through endocytic vesicles. *J. Cell Physiol.* **131**, 58-63.

Swarnakar, S., Beers, J., Strickland, D. K., Azhar, S. and Williams, D. L. (2001). The apolipoprotein E-dependent low density lipoprotein cholesteryl ester selective uptake pathway in murine adrenocortical cells involves chondroitin sulfate proteoglycans and an alpha 2-macroglobulin receptor. *J. Biol. Chem.* **276**, 21121-21128.

Van der Horst, D. J. (1990). Lipid transport function of lipoproteins in flying insects. *Biochim. Biophys. Acta* **1047**, 195-211.

Van der Horst, D. J., van Marrewijk, W. J. A. and Diederen, J. H. B. (2001). Adipokinetic hormones of insect: Release, signal transduction, and responses. *Int. Rev. Cytol.* **211**, 179-240.

Van der Horst, D. J., van Hoof, D., van Marrewijk, W. J. A. and Rodenburg, K. W. (2002). Alternative lipid mobilization: the insect shuttle system. *Mol. Cell. Biol.* (in press).

Vassiliou, G., Benoist, F., Lau, P., Kavaslar, G. N. and McPherson, R. (2001). The low density lipoprotein receptor-related protein contributes to selective uptake of high density lipoprotein cholesteryl esters by SW872 liposarcoma cells and primary human adipocytes. *J. Biol. Chem.* **276**, 48823-48830.

Verges, M., Havel, R. J. and Mostov, K. A. (1999). A tubular endosomal fraction from rat liver: biochemical evidence of receptor sorting by default. *Proc. Natl. Acad. Sci. USA* **96**, 10146-10151.

Weers, P. M. M., van Marrewijk, W. J. A., Beenakkers, A. M. T. and van der Horst, D. J. (1993). Biosynthesis of locust lipophorin. Apolipophorins I and II originate from a common precursor. *J. Biol. Chem.* **268**, 4300-4303.

Yamashiro, D. J., Tycko, B., Fluss, S. R. and Maxfield, F. R. (1984). Segregation of transferrin to a mildly acidic (pH 6.5) para-Golgi compartment in the recycling pathway. *Cell* **37**, 789-800.